npj | Quantum Materials

www.nature.com/npjquantmats

ARTICLE OPEN

Fe_3O_4 thin films: controlling and manipulating an elusive quantum material

Xionghua Liu[1], Chun-Fu Chang[1], Aurora Diana Rata[1,2], Alexander Christoph Komarek[1] and Liu Hao Tjeng[1]

Fe_3O_4 (magnetite) is one of the most elusive quantum materials and at the same time one of the most studied transition metal oxide materials for thin-film applications. The theoretically expected half-metallic behaviour generates high expectations that it can be used in spintronic devices. Yet, despite the tremendous amount of work devoted to preparing thin films, the enigmatic first-order metal–insulator transition, and the hallmark of magnetite known as the Verwey transition, is in thin films extremely broad and occurs at substantially lower temperatures as compared with that in high-quality bulk single crystals. Here we have succeeded in finding and making a particular class of substrates that allows the growth of magnetite thin films with the Verwey transition as sharp as in the bulk. Moreover, we are now able to tune the transition temperature and, using tensile strain, increase it to substantially higher values than in the bulk.

npj Quantum Materials (2016) **1,** 16027; doi:10.1038/npjquantmats.2016.27; published online 9 December 2016

INTRODUCTION

While thousands of studies have been devoted to trying to understand the first-order Verwey transition in magnetite, the high Curie temperature ($T_C \sim 860$ K) and the half-metallic character of Fe_3O_4 as predicted by band theory[1,2] have triggered considerable research efforts worldwide to make this material suitable for spintronic applications in the form of thin-film devices.[3–7] Using a variety of deposition methods, epitaxial growth on a number of substrates has been achieved.[5–8] Yet, it is remarkable that in the 20 years of research on Fe_3O_4 thin films, the first-order Verwey transition[9] in thin films is always broad.[6,7,10–13] Although in the bulk the transition takes place well within 1 K, the reported resistivity curves for the thin films showed transition widths of ~10 K or more. The Verwey transition temperature T_V in thin films is also much lower, with reported values ranging from 100 to 120 K,[6,7,10–13] whereas the stoichiometric bulk has T_V of 124 K.

It has been reported that several factors can affect negatively the Verwey transition in bulk magnetite, such as oxygen off-stoichiometry[14] and cation substitution.[15] The T_V gradually decreases and the transition is claimed to change from a first order to a second or even higher order with increasing oxygen off-stoichiometry or cation substitution. Recently, we have carried out a systematic study on the influence of oxygen stoichiometry for the properties of magnetite thin films,[16] and we found that even for the optimal oxygen composition the transition remains broad. In that study, we also discovered that the microstructure of the films has an important role. In particular, with the films having a distribution of domain sizes, a larger spread of the distribution results in a broader transition and a small domain size gives lower transition temperatures. The transition itself is still first order as it shows hysteresis, and there are indications that each domain has its own transition temperature.[16] Various substrates have been used in the literature to grow epitaxial Fe_3O_4 thin films, e.g., MgO, $MgAl_2O_4$, Al_2O_3, $SrTiO_3$ and $BaTiO_3$.[6,7,10–13,16] These studies may suggest that the larger the lattice mismatch, the broader the transition and the lower the average transition temperature.[16]

Here we have succeeded in finding and making a particular class of substrates that allows the growth of magnetite thin films with the Verwey transition as sharp as in the bulk. The key principle is to obtain thin films with sufficiently large domains and small domain size distribution. Moreover, using tensile strain, we now are able to increase the transition temperature to considerably higher values than that of the bulk. The occurrence of the Verwey transition in the highly anisotropic strained films raises a new question to the intricacies of the interplay between the charge and orbital degrees of freedom of the Fe ions in magnetite, adding another aspect of the elusiveness of this quantum material.

RESULTS

In our quest for substrates that allow for the growth of Fe_3O_4 thin films with large domains and a narrow distribution of domain sizes, we aim first of all for substrates with a very small lattice mismatch. Although MgO is ideal in this respect, the occurrence of anti-phase boundaries,[11] which cannot be avoided when growing a (inverse) spinel film on a rocksalt substrate, has a negative effect on the distribution and size of the domains.[16] We therefore restrict ourselves to substrates with the spinel structure. We have identified Co_2TiO_4 with a lattice mismatch of +0.66% as a potential candidate, and managed to prepare large single crystals of this compound using a mirror furnace. Substrates with ≈6 mm × 6 mm epi-polished surfaces have been made out of these crystals. We have also prepared crystals and substrates with somewhat larger lattice mismatch, up to +1.11%, by partial substitution of the Co with Mn and/or Fe: $Co_{1.75}Mn_{0.25}TiO_4$ and $Co_{1.25}Fe_{0.5}Mn_{0.25}TiO_4$. Details about the preparation and

[1]Max Planck Institute for Chemical Physics of Solids, Dresden, Germany.
Correspondence: XH Liu (Xionghua.Liu@cpfs.mpg.de) or LH Tjeng (Hao.Tjeng@cpfs.mpg.de)
[2]Current address: Institute of Physics, Martin Luther University, Halle-Wittenberg, 06099 Halle, Germany.
Received 11 July 2016; revised 21 October 2016; accepted 3 November 2016

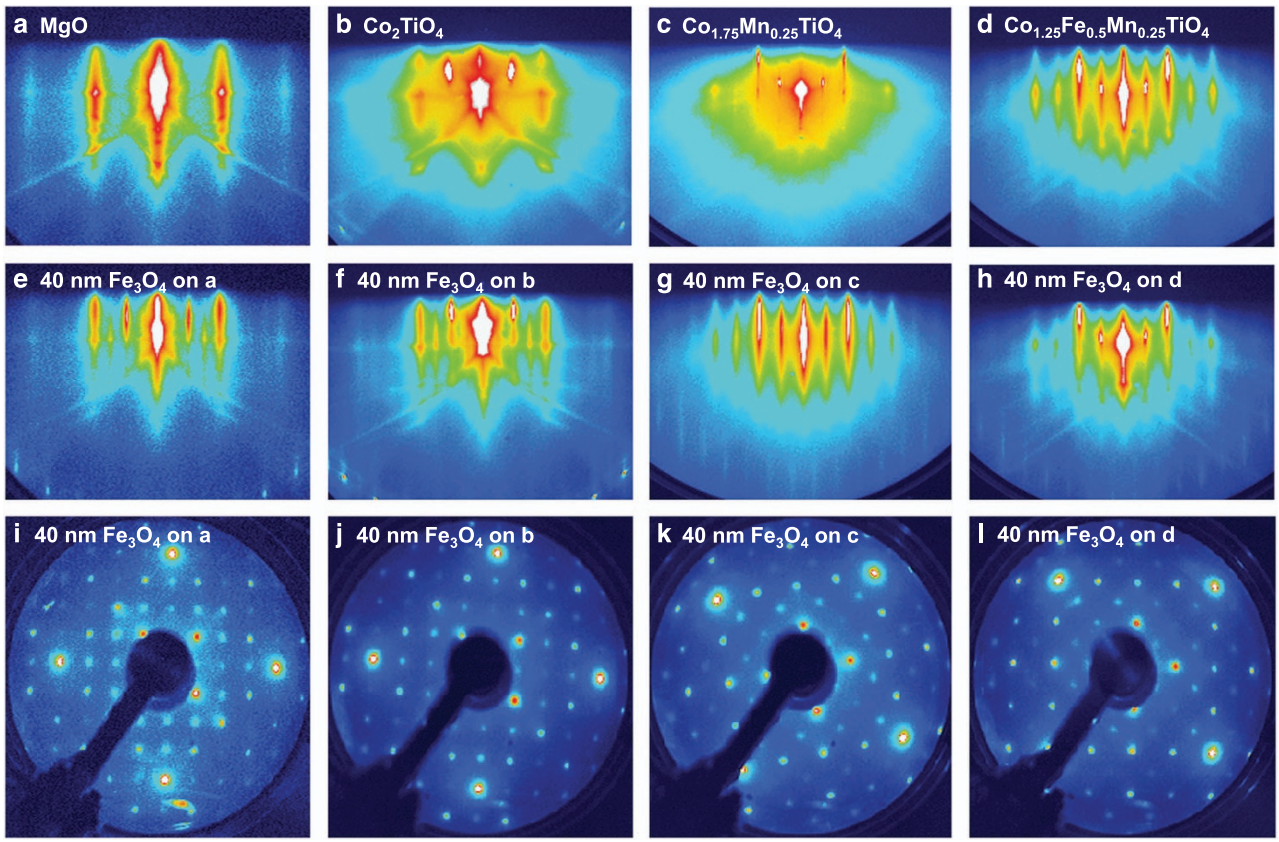

Figure 1. RHEED and LEED images. Representative RHEED patterns of clean (**a**) MgO (001), (**b**) Co_2TiO_4 (001), (**c**) $Co_{1.75}Mn_{0.25}TiO_4$ (001) and (**d**) $Co_{1.25}Fe_{0.5}Mn_{0.25}TiO_4$ (001) substrates. RHEED and LEED patterns, respectively, of 40 nm Fe_3O_4 films grown on MgO (001) (**e**,**i**), Co_2TiO_4 (001) (**f**,**j**), $Co_{1.75}Mn_{0.25}TiO_4$ (001) (**g**,**k**) and $Co_{1.25}Fe_{0.5}Mn_{0.25}TiO_4$ (001) (**h**,**l**).

properties of the substrate single crystals are given in Supplementary Information and Figures S1–S3).

Figure 1a–d displays the reflection high-energy electron diffraction (RHEED) patterns of the clean MgO (001), Co_2TiO_4 (001), $Co_{1.75}Mn_{0.25}TiO_4$ (001) and $Co_{1.25}Fe_{0.5}Mn_{0.25}TiO_4$ (001) substrates, respectively. Figure 1e–h shows the RHEED patterns and Figure 1i–l presents the low-energy electron diffraction (LEED) of the 40 nm-thick Fe_3O_4 films grown on these respective substrates. Details of the substrate cleaning procedure as well as of the growth conditions by using the molecular beam epitaxy technique can be found in the Materials and methods. The sharpness of the RHEED stripes and the presence of Kikuchi lines, as well as the high contrast and sharpness of the LEED spots indicate a flat and well-ordered single-crystalline (001) surface structure of the films. The presence of the $\left(\sqrt{2}\times\sqrt{2}\right)R45^\circ$ surface reconstruction pattern both in the RHEED and LEED images provides another indication for the high structural quality of the films. The valence states of the Fe ions were investigated by Fe 2*p* core level and valence band X-ray photoelectron spectroscopy (XPS), thereby showing the typical signatures of stoichiometric magnetite (Supplementary Figure S4). We also observe that the XPS spectra of the films grown on different substrates are identical, meaning that the substrate has no influence on the chemical composition of the films. We note that RHEED, LEED and XPS are surface-sensitive crystallographic and chemical techniques. We would like to refer to ref. 17 for a detailed discussion about the polar nature of the interface (and surface) and the consequences for the interface (and surface) crystal structure.

Figure 2a shows the temperature dependence of the resistivity of 40 nm-thick Fe_3O_4 films grown on MgO (001), Co_2TiO_4 (001), $Co_{1.75}Mn_{0.25}TiO_4$ (001) and $Co_{1.25}Fe_{0.5}Mn_{0.25}TiO_4$ (001), as well as that of a bulk single-crystal Fe_3O_4. We can clearly see that the bulk sample has a sharp Verwey transition at 124 K, whereas the film on MgO shows the typical broad transition at lower temperatures. In contrast, the thin films grown on the spinel substrates all show a very sharp transition, almost as sharp as the bulk. The hysteresis is all within 0.7 K. Most exciting is that now the transition temperatures of these thin films are even higher than that of the bulk. Defining T_{V+} (T_{V-}) as the temperature of the maximum slope of the ρ (T) curve for the warming up (cooling down) branch, the T_{V+} is 127 K for the film grown on Co_2TiO_4 (001) (lattice mismatch +0.66%), 133 K for the film on $Co_{1.75}Mn_{0.25}TiO_4$ (001) (+0.98%) and even 136 K for the film on $Co_{1.25}Fe_{0.5}Mn_{0.25}TiO_4$ (001) (+1.11%), which is 12 K higher than the T_{V+} of the bulk and ~15–35 K higher than the T_{V+} of films of similar thickness reported in the literature so far.[6,7,10–13,16]

Figure 2b plots T_{V+} as a function of the film thickness on the three variants of the spinel substrates, as well as that on the rocksalt MgO. The black horizontal line represents the T_{V+} of the bulk single crystal. We can observe that T_{V+} gradually increases with the film thickness, and again, that it is larger for the spinel substrates with the larger lattice constant mismatch between the film and the substrate. Although films with the thicknesses of 5 nm and less do not show a Verwey transition, we can clearly see a well-defined transition for films when they are 10 nm or thicker. In fact, we would like to note that films as thin as 10 nm grown on $Co_{1.75}Mn_{0.25}TiO_4$ (001) (+0.98%) and $Co_{1.25}Fe_{0.5}Mn_{0.25}TiO_4$ (001) (+1.11%) have a T_{V+} that is already comparable to that of the bulk, a highly remarkable result in view of the generally low values even for thicker films known in the literature.[6,7,10–13,16]

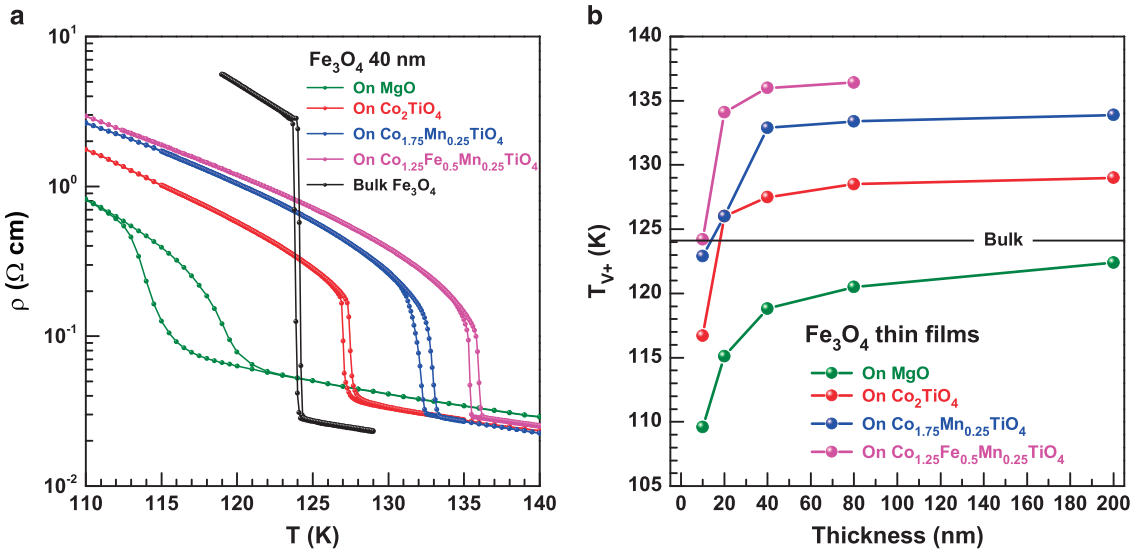

Figure 2. Electrical transport properties. (**a**) Resistivity as a function of temperature of 40 nm Fe_3O_4 thin films grown on MgO (001), Co_2TiO_4 (001), $Co_{1.75}Mn_{0.25}TiO_4$ (001) and $Co_{1.25}Fe_{0.5}Mn_{0.25}TiO_4$ (001) substrates and of single-crystal bulk Fe_3O_4. (**b**) The Verwey transition temperature (T_{V+}) as a function of film thickness of the films grown on MgO (001), Co_2TiO_4 (001), $Co_{1.75}Mn_{0.25}TiO_4$ (001) and $Co_{1.25}Fe_{0.5}Mn_{0.25}TiO_4$ (001) substrates, the black horizontal line represents the T_{V+} of a stoichiometric bulk magnetite crystal.

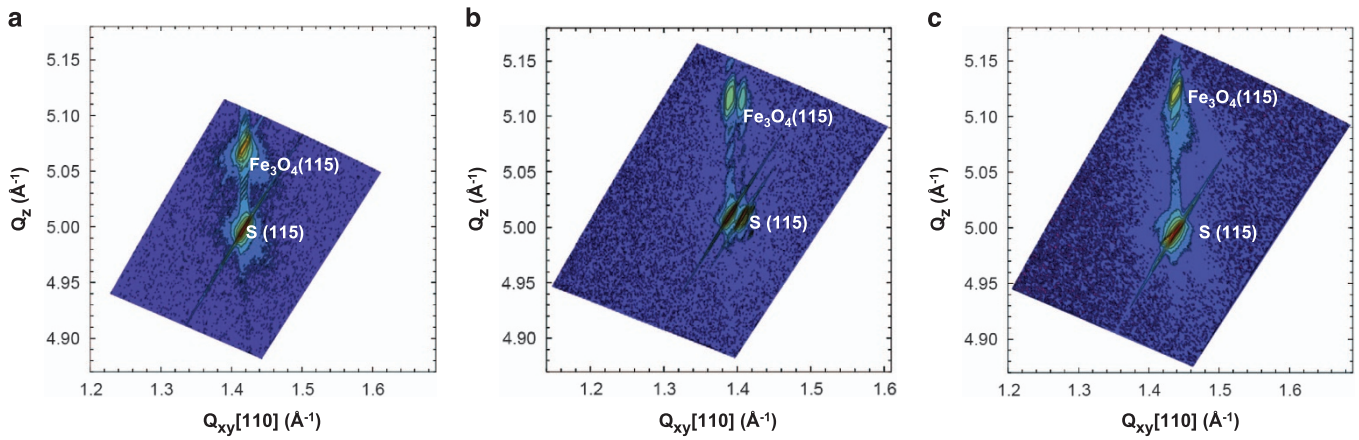

Figure 3. Reciprocal space maps. Reciprocal space mapping of the (1 1 5) reflection of (**a**) a 200 nm Fe_3O_4 film grown on Co_2TiO_4 (001) and of (**b**) a 40 nm Fe_3O_4 film grown on $Co_{1.75}Mn_{0.25}TiO_4$ as well as of (**c**) a 80 nm Fe_3O_4 film grown on $Co_{1.25}Fe_{0.5}Mn_{0.25}TiO_4$ (001).

We now investigate the strain state of the Fe_3O_4 films grown on the spinel substrates using X-ray diffraction (XRD). Figure 3 presents the reciprocal space mapping of the (115) reflection from a 200 nm-thick film grown on Co_2TiO_4 (001) (+0.66%; Figure 3a) and a 40 nm-thick film on $Co_{1.75}Mn_{0.25}TiO_4$ (+0.98%; Figure 3b) as well as from a 80 nm-thick film grown on $Co_{1.25}Fe_{0.5}Mn_{0.25}TiO_4$ (001) (+1.11%; Figure 3c). The well-aligned longitudinally (115) reflection of the film and the substrate demonstrates that the films are fully strained. Further, one observes clear thickness fringes along Q_z from the Fe_3O_4/Co_2TiO_4 film, see Figure 3a, which indicates a smooth surface and a uniform thickness of the film. A few less pronounced thickness fringes along Q_z are observed from the $Fe_3O_4/Co_{1.25}Fe_{0.5}Mn_{0.25}TiO_4$ film, see Figure 3c, which implies a rougher surface compared with that of the Fe_3O_4/Co_2TiO_4 film, giving rise to the intensity dispersion along the Q_z direction. We note that the $Co_{1.75}Mn_{0.25}TiO_4$ substrate is not perfect in the sense that it consists of two crystals misaligned by ~0.3° as can be seen by the double peak structure in the Q_{xy} direction. Yet, the film is still epitaxial and fully strained. Long range $\theta-2\theta$ XRD data indicate that there are no other phases than Fe_3O_4. We summarise the lattice constants of three variants of the spinel substrates, together with those of the 40, 80 and 200 nm Fe_3O_4 films grown on top of these substrates in Table 1 from the XRD measurements. As the lattice constant *a* of the substrates increases, i.e., 8.4528, 8.4797 and 8.4898 Å, the lattice constant *c* of the films gradually

Table 1. Lattice constants

	Substrate a	*40 nm* Fe_3O_4 c	*80 nm* Fe_3O_4 c	*200 nm* Fe_3O_4 c
Co_2TiO_4	8.4528 Å	8.3332 Å	8.3330 Å	8.3316 Å
$Co_{1.75}Mn_{0.25}TiO_4$	8.4797 Å	8.3042 Å	8.3048 Å	8.3054 Å
$Co_{1.25}Fe_{0.5}Mn_{0.25}TiO_4$	8.4898 Å	8.2800 Å	8.2806 Å	8.2855 Å

Lattice constants of 40, 80 and 200 nm Fe_3O_4 thin films on Co_2TiO_4, $Co_{1.75}Mn_{0.25}TiO_4$ and $Co_{1.25}Fe_{0.5}Mn_{0.25}TiO_4$.

decreases, e.g., 8.3332, 8.3042, 8.2800 Å, respectively, for the 40 nm films. To compare, the lattice constant of bulk Fe_3O_4 is 8.396 Å. From this, we calculate that the Poission ratio is in the range of 0.36–0.38, and that the volume increases as 595.29, 597.20 and 597.19 $Å^3$, respectively, for the 200 nm films, whereas the volume of bulk Fe_3O_4 is ~591.86 $Å^3$.

We can also get an insight about the microstructure of the films by analysing the peak profile of the rocking curves of the (115) reflection. From the inverse of the peak width, we can estimate that the average domain size is ~46, 61 and 68 nm for the 40 nm films grown on the three spinel substrates, respectively. These numbers are higher than the 30 nm value found for an equivalent thick film grown on MgO,[16] suggesting that the spinel structure of the substrate indeed does help to obtain films of structurally better quality. The complete set of data on the thickness dependence of the average domain size of the films grown on the spinels and MgO is given in Supplementary Figure S5. Combining this with the data in Figure 2b, we can deduce that as a function of thickness, the average domain size in the films increases and therefore also T_V, and that on the spinels the average domain size exceeds more quickly the value of ~60–80 nm beyond which the T_V reaches apparently its asymptotic value for a given strain situation. These results therefore support our conjecture that one needs films with sufficiently large domains and sufficiently narrow distribution of domain sizes to obtain sharp first-order transitions. Perhaps this is the solution to remedy the broad first-order transitions observed in, e.g., V_2O_3 thin films,[18–20] and $RENiO_3$ (RE = Pr, Nd, Sm) thin films,[18,21–24] e.g., one has to carefully design substrates with a matching lattice structure and sufficiently small lattice mismatch.

DISCUSSION

Having achieved magnetite thin films with a Verwey transition as sharp as the bulk, we now are ready to meaningfully measure and analyse the effect of the strain exerted by the substrate on the transition of the film. It has been reported that the Verwey transition of bulk magnetite becomes broad and that T_V drops linearly with increasing applied hydrostatic pressure and corresponding decrease of the unit cell volume.[25–28] Although the application of negative hydrostatic pressures is experimentally out of reach, our finding that the T_V of the Fe_3O_4 thin films increases when epitaxially grown with increasing unit cell volume indicates that we have in fact succeeded to exert effectively negative pressures on magnetite using the tensile strain imposed by the carefully chosen spinel substrates. Viewing the Verwey transition as a transition from a Wigner crystal to a Wigner glass of small polarons,[29] one can readily accept that changing the one-electron band width, and therefore also the polaron band width, will alter the transition temperature.[30] In particular, enlarging the lattice constant and inter-atomic distances will facilitate the formation of an ordered state in which the different lattice sites have different local valence and orbital states.

Yet it is important to note that the negative pressures exerted on these thin films are by no means isotropic and therefore cannot be considered as being the equivalent of negative hydrostatic pressures. On the contrary, the films are expanded in the plane but compressed along the *c* axis direction. This makes the Verwey transition in the tensile strained films even more interesting: would the charge and orbital order be of the same type as in the bulk, for which there is a lot of debate, see refs 31–33 and references therein. In this respect, we would like to note that the resistivity across the Verwey transition changes by about a factor 10 in the films, whereas it is by a factor 100 in the bulk. Clearly, the presence of the substrate limits a full opening of the conductivity gap by putting constraints on the crystal structure. Nevertheless, the transition does take place and so the question arises what are the minimal conditions required in terms of the local electronic structure such as the orbital state for such a transition to occur. It would be extremely interesting to address this question by, e.g., carrying out charge- and/or orbital-sensitive resonant XRD experiments, see ref. 33 and references therein. With the Verwey transition better defined and thus with the transport properties getting improved by the control of the domain size will provide confidence that high-quality spintronic devices can be made. In case for applications one needs to use a non-magnetic spinel substrate, then Mg_2TiO_4 (ref. 34) with a lattice constant of 8.44 Å is a good option.

MATERIALS AND METHODS

Fe_3O_4 thin films were grown using molecular beam epitaxy in an ultra-high vacuum chamber with a base pressure in the high 10^{-11} mbar range. High-purity Fe metal was evaporated from a LUXEL Radak effusion cell at temperatures of about 1,250 °C in a pure oxygen atmosphere onto single-crystalline Co_2TiO_4 (001), $Co_{1.75}Mn_{0.25}TiO_4$ (001) and $Co_{1.25}Fe_{0.5}Mn_{0.25}TiO_4$ (001) substrates. These substrates were annealed for 2 h at 400 °C in an oxygen pressure of 3×10^{-7} mbar to obtain a clean and well-ordered surface structure before the Fe_3O_4 deposition. The substrate temperature was kept at 250 °C in an oxygen pressure of 1×10^{-6} mbar during growth. The Fe flux was calibrated using a quartz-crystal monitor at the growth position before deposition and set to 1 Å min^{-1} for the growth of all films. *In situ* and real-time monitoring of the epitaxial growth was performed by RHEED measurements, which were taken at 20 keV electron energy, with the beam aligned parallel to the [100] direction of the substrate. The crystalline structure was also verified *in situ* after the growth by LEED, which was recorded at the electron energy of 88 eV. All samples were analysed *in situ* by XPS. The XPS data were collected using 1486.6 eV photons (monochromatised Al K_α light) in a normal emission geometry and at room temperature using a Scienta R3000 electron energy analyser. The overall energy resolution was set to be about 0.3 eV. XRD was employed for further *ex situ* investigation of the structural quality and the microstructure of the films. The XRD measurements were performed with a high-resolution PANalytical X'pert MRD diffractometer (PANalytical, Almelo, The Netherlands) using monochromatic Cu $K_{\alpha1}$ radiation ($\lambda = 1.54056$ Å). Temperature-dependent resistivity (ρ) measurements of the Fe_3O_4 thin films were performed by the standard four probe technique using a Physical Property Measurement System. The ρ–T curves for all the samples were measured with a current source of 0.1 μA from 300 to 80 K and back to 300 K at zero field.

ACKNOWLEDGEMENTS

We acknowledge valuable comments from S. Wirth. The research of XHL was supported by the Max Planck-POSTECH Center for Complex Phase Materials.

CONTRIBUTIONS

X.H.L. grew and characterised the films with the help from C.F.C. and A.D.R. X.H.L. carried out the electrical transport and magnetic properties measurements. A.C.K. grew and characterised the substrates and the bulk Fe_3O_4 crystals. X.H.L., C.F.C. and L.H.T. performed the data analysis and wrote the manuscript.

COMPETING INTERESTS

The authors declare no conflict of interest.

REFERENCES

1. de Groot, R. A., Müller, F. M., van Engen, P. G. & Buschow, K. H. J. New class of materials: half-metallic ferromagnets. *Phys. Rev. Lett.* **50**, 2024–2027 (1983).
2. Yanase, A. & Siratori, K. Band structure in the high temperature phase of Fe_3O_4. *J. Phys. Soc. Jpn* **53**, 312–317 (1984).
3. Li, X. W., Gupta, A., Xiao, G., Qian, W. & Dravid, V. P. Fabrication and properties of heteroepitaxial magnetite (Fe_3O_4) tunnel junctions. *Appl. Phys. Lett.* **73**, 3282–3284 (1998).
4. Greullet, F. *et al.* Large inverse magnetoresistance in fully epitaxial Fe/Fe_3O_4/MgO/Co magnetic tunnel junctions. *Appl. Phys. Lett.* **92**, 053508 (2008).
5. Chambers, S. A. Epitaxial growth and properties of thin film oxides. *Surf. Sci. Rep.* **39**, 105–180 (2000).

6. Ziese, M. Extrinsic magnetotransport phenomena in ferromagnetic oxides. *Rep. Prog. Phys.* **65**, 143–249 (2002).
7. Moussy, J. B. From epitaxial growth of ferrite thin films to spin-polarized tunnelling. *J. Phys. D Appl. Phys.* **46**, 143001 (2013).
8. Mijiritskii, A. V. & Boerma, D. O. The (001) surface and morphology of thin Fe_3O_4 layers grown by O_2-assisted molecular beam epitaxy. *Surf. Sci.* **486**, 73–81 (2001).
9. Verwey, E. J. W. Electronic conduction of magnetite (Fe_3O_4) and its transition point at low temperatures. *Nature* **144**, 327–328 (1939).
10. Gong, G. Q., Gupta, A., Xiao, G., Qian, W. & Dravid, V. P. Magnetoresistance and magnetic properties of epitaxial magnetite thin films. *Phys. Rev. B* **56**, 5096–5099 (1997).
11. Eerenstein, W., Palstra, T. T. M., Hibma, T. & Celotto, S. Origin of the increased resistivity in epitaxial Fe_3O_4 films. *Phys. Rev. B* **66**, 201101(R) (2002).
12. Arora, S. K., Sofin, R. G. S. & Shvets, I. V. Magnetoresistance enhancement in epitaxial magnetite films grown on vicinal substrates. *Phys. Rev. B* **72**, 134404 (2005).
13. Geprags, S., Mannix, D., Opel, M., Goennenwein, S. T. B. & Gross, R. Converse magnetoelectric effects in $Fe_3O_4/BaTiO_3$ multiferroic hybrids. *Phys. Rev. B* **88**, 054412 (2013).
14. Aragon, R., Gehring, P. M. & Shapiro, S. M. Stoichiometry, percolation, and Verwey ordering in magnetite. *Phys. Rev. Lett.* **70**, 1635–1638 (1993).
15. Brabers, V. A. M., Walz, F. & Kronmüller, H. Impurity effects upon the Verwey transition in magnetite. *Phys. Rev. B* **58**, 14163–14166 (1998).
16. Liu, X. H., Rata, A. D., Chang, C. F., Komarek, A. C. & Tjeng, L. H. Verwey transition in Fe_3O_4 thin films: Influence of oxygen stoichiometry and substrate-induced microstructure. *Phys. Rev. B* **90**, 125142 (2014).
17. Chang, C. F. *et al.* Dynamic atomic reconstruction: how Fe_3O_4 thin films evade polar catastrophe for epitaxy. *Phys. Rev. X* **6**, 041011 (2016).
18. Imada, M., Fujimori, A. & Tokura, Y. Metal-insulator transitions. *Rev. Mod. Phys.* **70**, 1039–1263 (1998).
19. Brockman, J., Samant, M. G., Roche, K. P. & Parkin, S. S. P. Substrate-induced disorder in V_2O_3 thin films grown on annealed c-plane sapphire substrates. *Appl. Phys. Lett.* **101**, 051606 (2012).
20. Sakai, J., Limelette, P. & Funakubo, H. Transport properties and c/a ratio of V_2O_3 thin films grown on C- and R-plane sapphire substrates by pulsed laser deposition. *Appl. Phys. Lett.* **107**, 241901 (2015).
21. Hepting, M. *et al.* Tunable charge and spin order in $PrNiO_3$ thin films and superlattices. *Phys. Rev. Lett.* **113**, 227206 (2014).
22. Mikheev, E. *et al.* Tuning bad metal and non-Fermi liquid behavior in a Mott material: Rare-earth nickelate thin films. *Sci. Adv.* **1**, 1500797 (2015).
23. Zhang, J. Y., Kim, H., Mikheev, E., Hauser, A. J. & Stemmer, S. Key role of lattice symmetry in the metal-insulator transition of $NdNiO_3$ films. *Sci. Rep* **6**, 23652 (2016).
24. Shi, J., Ha, S. D., Zhou, Y., Schoofs, F. & Ramanathan, S. A correlated nickelate synaptic transistor. *Nat. Commun.* **4**, 2676 (2013).
25. Nakagiri, N., Manghnani, M. H., Ming, L. C. & Kimura, S. Crystal structure of magnetite under pressure. *Phys. Chem. Minerals* **13**, 238–244 (1986).
26. Ramasesha, S. K., Mohan, M., Singh, A. K., Honig, J. M. & Rao, C. N. R. High-pressure study of Fe_3O_4 through the Verwey transition. *Phys. Rev. B* **50**, 13789–13791 (1994).
27. Rozenberg, G. K., Hearne, G. R., Pasternak, M. P., Metcalf, P. A. & Honig, J. M. Nature of the Verwey transition in magnetite (Fe_3O_4) to pressures of 16 GPa. *Phys. Rev. B* **53**, 6482–6487 (1996).
28. Brabers, J. H. V. J., Walz, F. & Kronmüller, H. The role of volume effects in the Verwey transition in magnetite. *J. Phys. Condens. Matter* **11**, 3679–3686 (1999).
29. Mott, N. F. Electrons in disordered structures. *Adv. Phys.* **16**, 49–144 (1967).
30. Cullen, J. R. & Callen, E. R. Multiple ordering in magnetite. *Phys. Rev. B* **7**, 397–402 (1973).
31. Wright, J. P., Attfield, J. P. & Radaelli, P. G. Long range charge ordering in magnetite below the Verwey transition. *Phys. Rev. Lett.* **87**, 266401 (2001).
32. Senn, M. S., Wright, J. P. & Attfield, J. P. Charge order and three-site distortions in the Verwey structure of magnetite. *Nature* **481**, 173–176 (2012).
33. Tanaka, A. *et al.* Analysis of charge and orbital order in Fe_3O_4 by Fe $L_{2,3}$ resonant x-ray diffraction. *Phys. Rev. B* **88**, 195110 (2013).
34. Hohl, H., Kloc, C. & Bucher, E. Electrical and magnetic properties of spinel solid solutions $Mg_{2-x}Ti_{1+x}O_4$; $0 \le x \le 1$. *J. Solid State Chem.* **125**, 216–223 (1996).

Supplementary Information accompanies the paper on the *npj Quantum Materials* website (http://www.nature.com/npjquantmats)